http://dx.doi.org/10.5012/bkcs.2013.34.2.465

Ultrafast Excited State Intramolecular Proton Transfer Dynamics of 1-Hydroxyanthraquinone in Solution

Jaehyun Ryu, Hyun Woo Kim,† Myung Soo Kim,‡ and Taiha Joo*

*Department of Chemistry, Pohang University of Science and Technology, Pohang 790-784, Korea. *E-mail: thjoo@postech.ac.kr*
†Institute of Theoretical and Computational Chemistry, Department of Chemistry, Pohang University of Science and Technology, Pohang 790-784, Korea
‡Department of Chemistry, Seoul National University, Seoul 151-742, Korea
Received November 1, 2012, Accepted November 16, 2012

Proton transfer reaction is one of the most fundamental processes in chemistry and life science. Excited state intramolecular proton transfer (ESIPT) has been studied as a model system of the proton transfer, since it can be conveniently initiated by light. We report ESIPT reaction dynamic of 1-hydroxy-anthraquione (1-HAQ) in solution by highly time-resolved fluorescence. ESIPT time of 1-HAQ is determined to be 45 ± 10 fs directly from decay of the reactant fluorescence and rise of the product fluorescence. High time resolution allows observation of the coherent vibrational wave packet motion in the excited state of the reaction product tautomer. The coherently excited vibrational mode involves large displacement of the atoms, which shortens the distance between the proton donor and the acceptor. With the theoretical analysis, we propose that the ESIPT of 1-HAQ proceeds barrierlessly with assistance of the skeletal vibration, which in turn becomes excited coherently by the ESIPT reaction.

Key Words : ESIPT, Time-resolved fluorescence, Coherent nuclear wave-packet

Introduction

Excited state intramolecular proton transfer (ESIPT) has been studied as a model system of the proton transfer reaction, which is one of the most fundamental processes in chemistry as well as in life science.[1,2] At first, proton transfer was recognized as a tunneling process on a double well potential.[3] For the tunneling to be the main reaction pathway, there should be a sufficient barrier on the reactive potential energy surface (PES). Recently, however, for typical ESIPT molecules such as 2-(2'-hydroxyphenyl)benzothiazole and 10-hydroxybenzo[*h*]quinoline that undergo ultrafast ESIPT, coherent excitations of low frequency skeletal vibrations on the PES of the reaction product have been reported by femtosecond spectroscopies.[4-7] Based on those experiments, a multi-dimensional picture for the PES of the ESIPT was proposed.[8-10] In this model, vibrational modes involving large amplitude skeletal deformation shorten the distance between the proton and the proton acceptor, and promote the proton transfer. As a result, these vibrational modes are coherently excited on the product state.

Keto-enol tautomerism and their ESIPT reaction dynamics of the derivatives of hydroxyanthraquinone have been studied by stationary and time-resolved spectroscopies.[11-18] Smith *et al.* investigated the ESIPT of anthraquinone derivatives by using time-resolved fluorescence (TRF) and transient absorption (TA).[13] An ESIPT time of 100-300 fs was noted, and tunneling of the localized proton nuclear wave packet was invoked to account for the fast proton transfer. Choi *et al.* reported that ESIPT of 1-hydroxy-anthraquione (1-HAQ) in toluene occurs in 120 fs[18] (260 fs[17]). Molecular structures and the ESIPT scheme of 1-HAQ are shown in Figure 1. Delocalization of the proton nuclear wave packet (rapid collapse of the initial Franck-Condon state) within the double well PES was stated. Based on these experimental results, quantum mechanical calculations on the excited state PES responsible for the ESIPT was reported.[19] Interestingly, however, ESIPT of 1-HAQ was predicted not to occur, because the tautomer form has a higher energy than that of the normal form in the excited state.[19] In another report, opposite result was found from a quantum mechanical calculation employing density functional theory (DFT) method.[12] For 1,8-dihydroxyanthraquinone (DAQ), an analog of 1-HAQ, instrument limited rise of the tautomer emission was observed in a TRF experiment at 170 fs time-resolution.[20] Although the experiments reported instrument limited rise of the tautomer emission, actual reaction time was not resolved due to the insufficient time-resolution. Moreover, spectral relaxation processes such as solvation and vibronic relaxation may also contribute to the time-resolved signal, which may interfere with the measurements.

It has been shown that accurate reaction rate is one of the most important parameter to determine the molecular reaction dynamics of ESIPT.[5] When an ESIPT is ultrafast, the reaction itself can act as impulsive excitations of the vib-

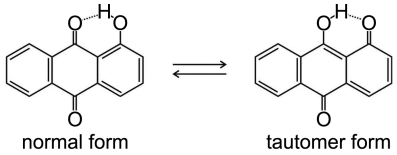

Figure 1. Molecular structure of 1-HAQ and ESIPT scheme.

rations on the product PES. Observation of such coherent wave packet motion together with the precise reaction rate can determine the occurrence of the ESIPT reaction and its molecular reaction dynamics. In this work, we employ TRF with high enough time resolution to resolve the ESIPT dynamics of 1-HAQ directly in time and to observe the coherent wave packet motion of the tautomer in the excited state. Although TA has been used exclusively for high time resolution, the coherent spike in a TA signal emerging around time zero significantly masks early dynamics,[21] since TA is based on the third order nonlinear process. In addition, excited state absorption, ground state bleach,[22] and product absorption contributions of a TA signal may complicate the analysis.

Experimental

The TRF apparatus employing fluorescence up-conversion method in a noncollinear sum frequency generation (SFG) geometry has been described in detail elsewhere.[23] To achieve the time resolution of ~30 fs required for the observation of the coherent vibrational wave packet motion of the tautomer in the excited state, 1-HAQ was excited by two photon absorption (TPA) process.[24] Femtosecond pulses at 810 nm were generated by a home-built cavity dumped Ti:sapphire laser pumped by a frequency doubled Nd:YVO_4 laser (Verdi, Coherent Inc.), and cavity-dumped at the repetition rate of 975 kHz. The 810 nm pulses were beam-split in 2:1 ratio, and used as the pump and gate pulses, respectively. Polarizations of the pump and the gate pulses were set to the magic angle (54.7°). The pump pulses were focused to a sample solution in a 200 μm thick flow cell by a 19 mm focal length lens. At the sample position, the pulse energy was 5 nJ and the beam diameter was estimated to be 10 μm. A 100 μm thick β-barium borate (BBO) crystal was used for the SFG of the fluorescence and the gate pulses. The SFG signal was dispersed by a monochromator (DH-10, Horiba) and detected by a photomultiplier tube and a gated photon counter (SR400, Stanford Research). Instrument response function (IRF) of the TRF apparatus was estimated by the cross-correlation between the gate and the scattered 405 nm light generated by inserting a thin BBO crystal at the sample position. IRF of 37 fs (full width at half maximum) was obtained, which sets the upper limit, since the effect of group velocity mismatch is smaller at longer wavelengths. Actual time-resolution depends on the detection wavelengths; it is estimated to be ~30 fs at 600 nm.[24]

1-HAQ (TCI) and toluene (Aldrich, spectroscopic grade) were used as received. Sample solution of 1 mM was prepared, which gave absorbance of 0.7 in the 200 μm flow cell. All measurements were carried out at ambient temperature (23 ± 1 °C).

Results and Discussion

The steady-state absorption and emission spectra of 1-HAQ are shown in Figure 2. Toluene was used as a solvent,

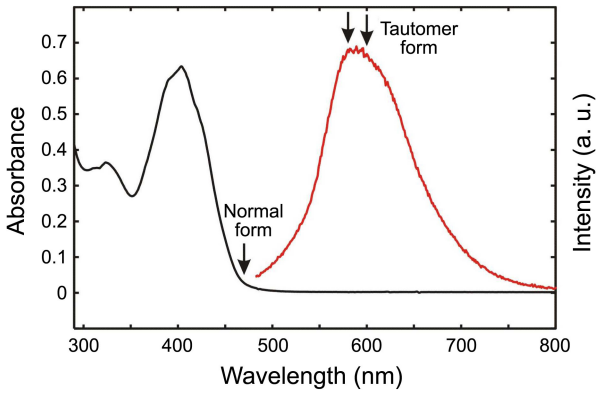

Figure 2. Steady-state absorption (black) and emission (red) spectra of 1-HAQ in toluene. Arrows indicate the detection wavelengths in the TRF measurements.

because 1-HAQ in a polar protic solvent is known to exist as an equilibrium mixture in the ground state.[14] Intermolecular hydrogen bonding with a protic solvent may also be present, which gives a proton transfer dynamics different from that of the intramolecular hydrogen bonded species.[25] For the nonprotic solvent, 1-HAQ in the ground state exists as the normal form with intramolecular hydrogen bonding almost exclusively, that is, the absorption band showing maximum at 404 nm is due to the normal form.[11] The Stokes shift is large, nearly 8000 cm^{-1}, and the fluorescence from the normal form is nearly absent indicating ultrafast ESIPT.

TRF signals of 1-HAQ in toluene detected at 470 and 600 nm are shown in Figure 3. Interference from the solvent

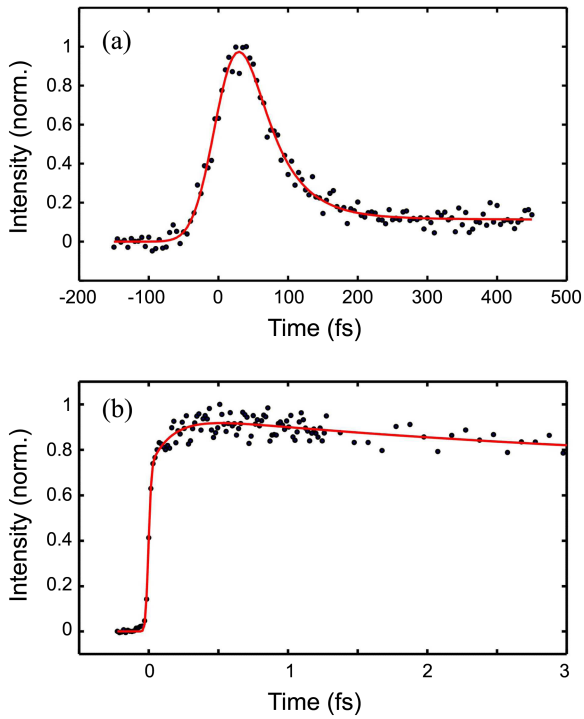

Figure 3. TRF signals of 1-HAQ in toluene detected at the normal form emission at 470 nm (a) and the tautomer form at 600 nm (b). The red lines indicate exponential fits. The sample was excited by 810 nm pulses *via* TPA process.

Raman signal is negligible as checked with the blank solvent. The TRF at 470 nm arises from the normal form predominantly, whereas the TRF at 600 nm arises from the tautomer form exclusively. The TRF signals were fitted to a sum of exponentials, and the results are summarized in Table 1. Fluorescence from the normal form shows ultrafast decay of 45 ± 10 fs. Corresponding rise was observed in the TRF at 600 nm, where the tautomer form emits. We assign the decay time constant of the normal form emission as the ESIPT time, since the rise time of the tautomer emission is not well determined due to the oscillations arising from the nuclear wave packet motion of the tautomer in the excited state (*vide infra*). The small long time component observed in the 470 nm TRF is believed to be due to the tautomer emission. The 160 fs rise component at 600 nm can be assigned to the vibronic relaxation and/or solvation process, although the origin of the 3.9 ps component is uncertain.

The ultrafast ESIPT time of 45 fs for 1-HAQ is consistent with the previous reports,[17,18,20] where instrument limited rise of the tautomer emission was observed. Also it is similar to the ESIPT rate found for 2-(2'-hydroxyphenyl) benzothiazole,[5,7] where proton acceptor is the nitrogen atom. Ultrafast yet finite ESIPT time of 45 fs is a valuable information to account for the ESIPT dynamics; it is immediately apparent that this result is inconsistent with the proposal that the initial Franck-Condon state is prepared above the barrier of the double-well potential and collapses instantly.[20] We have calculated energy of the excited state along the OH coordinate quantum mechanically by using CIS method and 6-31+G* basis. A transition barrier of 2.19 kcal/mol was obtained. Although the reaction barrier small, direct proton transfer along the OH coordinate may not occur in 45 fs.

Table 1. Nonlinear least-square exponential fit results of the TRF signals. A sum of exponentials convoluted with a Gaussian pulse was used for the fit. A negative amplitude indicates a rise

λ (nm)	A_1	τ_1 (fs)	A_2	τ_2 (fs)	A_3	τ_3 (ps)	A_3	τ_4
470	0.92	45	0.08	∞[a]				
600	-0.73	40	-0.27	160	0.26	3.9	0.74	∞[a]

[a]Long time constant that cannot be determined accurately.

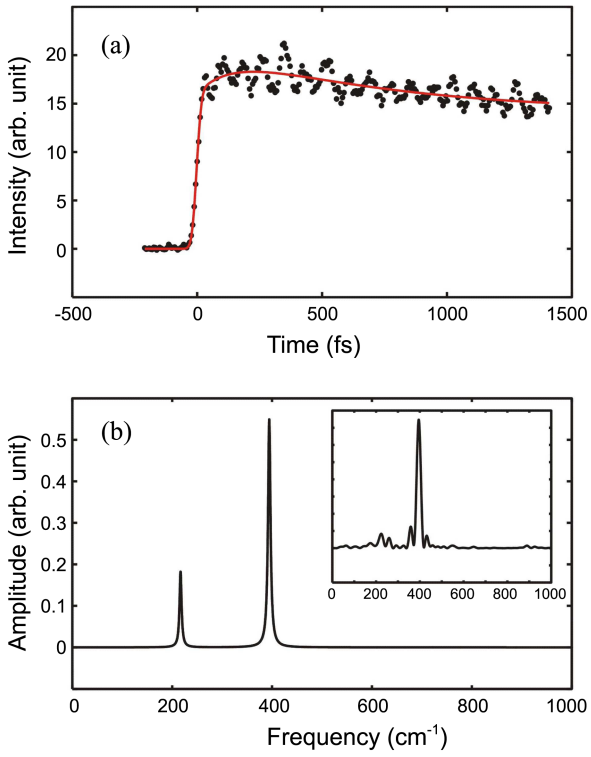

Figure 4. TRF signals of the tautomer form detected at 580 nm. The red line represents the exponential fit. (b) Oscillation spectrum in the TRF signals obtained by LPSVD. Inset shows the FFT power spectrum.

When half of the vibrational period is regarded as a measure of impulsive excitation, vibrational modes with frequencies below ~370 cm^{-1}, whose period of vibration is 90 (2 × 45) fs, can be excited impulsively. Figure 4(a) shows the TRF at 580 nm where the tautomer emits. The 580 nm detection wavelength was selected, because the amplitudes of oscillations are higher than those at the emission maximum. In addition to the fast rise, extensive oscillations are evident. These oscillations in the TRF of the reaction product arise, since the ESIPT reaction can act as impulsive excitations to some low frequency vibrations. Linear prediction singular value decomposition (LPSVD)[26] and fast Fourier transform (FFT) methods were used to analyze the signals. LPSVD results are listed in Table 2. This represents the first experimental observation of the nuclear wave packet dynamics of 1-HAQ, which was made possible by the time resolution shorter than certain vibrational periods.

To account for the oscillatory components appeared in time resolved signals, we first assumed that the ESIPT occurs instantaneously. Then, we treat the ESIPT reaction as a Franck-Condon transition to define the general Huang-Rhys factors (S) for the chemical reaction

$$S = \frac{d^2 m\omega}{2\hbar}, \tag{1}$$

where d is the displacement along the reaction for the vibrational mode with frequency ω and reduced mass m. The normal-mode projected displacements δ were calculated by projecting the geometry change between the reactant and the product onto the normal modes of the product state[27]

$$\delta = -L_P^{-1} c_P^T m^{1/2} (x_P^0 - x_R^0). \tag{2}$$

Here L is the diagonal matrix with $L_{ii} = \sqrt{\hbar/\omega_i}$, c is the normal mode matrix, and x_k^0 is the geometry vector of the state k. Subscripts P and R denote reactant and product,

Table 2. Oscillation components in the TRF signals of the tautomer form monitored at 580 nm. T_2 and ϕ are the vibrational dephasing time and phase, respectively

Amplitude	ω (cm^{-1})	T_2 (ps)	ϕ (deg.)
0.22	217	2.2	-143
0.81	394	1.8	-48

respectively. Vibrational reorganization energy for the reaction can also be calculated

$$\lambda_i = \hbar\omega\delta^2/2 . \quad (3)$$

In this picture, vibrational modes with large *S* will be excited preferentially by the chemical reaction; vibrational mode with a large displacement will be excited in a Franck-Condon transition. The amplitude of oscillation for a vibrational mode in the TRF signal should be proportional to λ in the limit of delta function IRF. For a finite IRF, the amplitude will be attenuated by $\exp(-\sigma^2\omega^2/2)$, where s is the standard deviation of the IRF assuming Gaussian.[28] For example, oscillation amplitude of 417 cm^{-1} mode will be attenuated by a factor of 2 due to the finite time-resolution of the measurement.

Quantum mechanical calculations were performed to obtain the geometry change vector between the ground 1-HAQ (reactant) and the tautomer in the excited state (product) by the DFT and CIS methods, respectively. Gaussian 03 package[29] was used with 6-31+G(d,p) basis set. Vibrational modes below 500 cm^{-1} with non-zero Huang-Rhys factors and the vibrational reorganization energies are listed in Table 3 (full list is found in the supporting information). The two bands at 217 and 394 cm^{-1} observed in the experiments can be safely assigned to the ν_6 and ν_{11} modes, respectively. Interestingly, the two modes are the in-plane skeletal deformations that involve large displacement of the oxygen atoms to shorten the distance between the proton and the acceptor oxygen atom (see supporting information). Especially, ν_{11} involves symmetric displacements of the quinone oxygens predominantly. Therefore, we can conjecture that n_{11} mode may play a significant role for the ESIPT reaction. Although there are many vibrations below 500 cm^{-1} that supposed to be excited according to the model, only the two modes were observed experimentally. The discrepancy may arise from the assumption of the instantaneous ESIPT. It was shown by molecular dynamics simulations that vibrational excitations in an ultrafast chemical reaction may depend strongly on the detailed pathway of the reaction on the excited PES.[30,31]

For the barrierless reaction, roughly half of the vibrational period along the reaction coordinate can be regarded as the reaction rate. Since the reaction rate is $(45\ fs)^{-1}$, we can deduce the frequency of the vibrational mode that may be regarded as a reaction coordinate, which is 370 cm^{-1}. In addition, considering the criterion of the impulsive excitation, vibrational modes with frequencies below ~370 cm^{-1} can be excited impulsively. Since the highest frequency that was observed experimentally was 394 cm^{-1}, which is close to the upper limit of impulsive excitation, one can consider the ν_{11} as the mode that contribute significantly. That is, the skeletal deformation along the ν_{11} vibrational mode may induce the reaction barrierless. Therefore, we propose that the ESIPT of 1-HAQ proceeds through the assistance of mostly ν_{11} skeletal vibration. The ν_{11} mode, whose vibrational period is ~85 fs, shortens the distance between the proton and the oxygen accepting proton to make the reaction barrierless. Prompt hop of the proton is followed within half of the ν_{11} vibrational period. This conclusion is in line with the skeletal deformation model proposed by Schriever *et al.*[9]

Table 3. Calculated vibrational modes of the excited state tautomer below 500 cm^{-1} showing non-zero Huang-Rhys factor (*S*) and vibrational reorganization energies (λ). A scale factor of 0.9538 was used to obtain the fundamental vibrational frequencies (ω) from the CIS calculation[32]

vib. mode	ω (cm^{-1})	S	λ (cm^{-1})
6A'	225	0.0034	0.8
8A'	321	0.20	66
9A'	354	0.44	163
11A'	396	0.36	148
12A'	404	0.64	272
15A'	481	0.050	25

Conclusions

In this work, ESIPT reaction dynamic of 1-HAQ was studied by both spectroscopic tools and theoretical calculations. The ultrafast ESIPT reaction time of 1-HAQ was determined to be 45 ± 10 fs directly from the decay of the reactant fluorescence. Coherent vibrational wave packet dynamics of 1-HAQ in the excited state of the tautomer was observed directly through the modulation of the spontaneous fluorescence signal in time. The dominant vibrational mode that was excited impulsively is a skeletal vibration that involves large displacement of the quinone oxygen atoms, by which the reaction becomes barrierless. More importantly, we have demonstrated that time-resolved spontaneous fluorescence acquired with extreme time resolution combined with quantum mechanical calculation is a powerful tool that gives detailed information on the molecular reaction dynamics.

Acknowledgments. This work was supported by the National Research Foundation of Korea (NRF) grant funded by the Korea government (MEST) (2007-0056330) and the Global Research Laboratory Program (2009-00439).

References

1. Ernsting, N. P. *J. Phys. Chem.* **1985**, *89*, 4932.
2. Elsaesser, T.; Kaiser, W. *Chem. Phys. Lett.* **1986**, *128*, 231.
3. Weller, A. *Prog. React. Kinet.* **1961**, *1*, 188.
4. Takeuchi, S.; Tahara, T. *J. Phys. Chem. A* **2005**, *109*, 10199.
5. Kim, C. H.; Joo, T. *Phys. Chem. Chem. Phys.* **2009**, *11*, 10266.
6. Lochbrunner, S.; Stock, K.; Riedle, E. *J. Mol. Struct.* **2004**, *700*, 13.
7. Lochbrunner, S.; Wurzer, A. J.; Riedle, E. *J. Chem. Phys.* **2000**, *112*, 10699.
8. Lochbrunner, S.; Wurzer, A. J.; Riedle, E. *J. Phys. Chem. A* **2003**, *107*, 10580.
9. Schriever, C.; Barbatti, M.; Stock, K.; Aquino, A. J. A.; Tunega, D.; Lochbrunner, S.; Riedle, E.; de Vivie-Riedle, R.; Lischka, H. *Chem. Phys.* **2008**, *347*, 446.
10. Schriever, C.; Lochbrunner, S.; Ofial, A. R.; Riedle, E. *Chem. Phys. Lett.* **2011**, *503*, 61.
11. Marzocchi, M. P.; Mantini, A. R.; Casu, M.; Smulevich, G. *J. Chem. Phys.* **1998**, *108*, 534.

12. Cho, S. H.; Huh, H.; Kim, H. M.; Kim, C. I.; Kim, N. J.; Kim, S. K. *J. Chem. Phys.* **2005**, *122*, 034304.
13. Smith, T. P.; Zaklika, K. A.; Thakur, K.; Walker, G. C.; Tominaga, K.; Barbara, P. F. *J. Phys. Chem.* **1991**, *95*, 10465.
14. Fain, V. Y.; Zaitsev, B. E.; Ryabov, M. A. *Russ. J. Org. Chem.* **2006**, *42*, 1469.
15. Cho, D. W.; Kim, S. H.; Yoon, M.; Jeoung, S. C. *Chem. Phys. Lett.* **2004**, *391*, 314.
16. Cho, D. W.; Song, K. D.; Park, S. K.; Jeon, K. S.; Yoon, M. *Bull. Korean Chem. Soc.* **2007**, *28*, 647.
17. Choi, J. R.; Jeoung, S. C.; Cho, D. W. *Bull. Korean Chem. Soc.* **2003**, *24*, 1675.
18. Choi, J. R.; Jeoung, S. C.; Cho, D. W. *Chem. Phys. Lett.* **2004**, *385*, 384.
19. Yi, P. G.; Liang, Y. H. *Chem. Phys.* **2006**, *322*, 382.
20. Arzhantsev, S. Y.; Takeuchi, S.; Tahara, T. *Chem. Phys. Lett.* **2000**, *330*, 83.
21. Park, J. S.; Joo, T. *J. Chem. Phys.* **2004**, *120*, 5269.
22. Wise, F. W.; Rosker, M. J.; Tang, C. L. *J. Chem. Phys.* **1987**, *86*, 2827.
23. Rhee, H.; Joo, T. *Opt. Lett.* **2005**, *30*, 96.
24. Kim, C. H.; Joo, T. *Opt. Express* **2008**, *16*, 20742.
25. Kim, C. H.; Chang, D. W.; Kim, S.; Park, S. Y.; Joo, T. *Chem. Phys. Lett.* **2008**, *450*, 302.
26. Barkhuijsen, H.; De Beer, R.; Bovee, W. M. M. J.; Van Ormondt, D. *J. Magn. Reson.* **1985**, *61*, 465.
27. Reimers, J. R. *J. Chem. Phys.* **2001**, *115*, 9103.
28. Kim, S. Y.; Kim, C. H.; Park, M.; Ko, K. C.; Lee, J. Y.; Joo, T. *J. Phys. Chem. Lett.* **2012**, *3*, 2761.
29. Frisch, M. J. *et al.* Gaussian 03, Revision C.02; Gaussian, Inc.: Wallingford, CT, 2003.
30. Park, J. W.; Kim, H. W.; Song, C.-I.; Rhee, Y. M. *J. Chem. Phys.* **2011**, *135*, 014107.
31. Higashi, M.; Saito, S. *J. Phys. Chem. Lett.* **2011**, *2*, 2366.
32. Merrick, J. P.; Moran, D.; Radom, L. *J. Phys. Chem. A* **2007**, *111*, 11683.